POLITECNICO
MILANO 1863

SCUOLA DI INGEGNERIA INDUSTRIALE
E DELL'INFORMAZIONE

Executive Summary of the Thesis

Design and Hysteresis Compensation of a Robot-assisted System for Transesophageal Echocardiography

Laurea Magistrale in Biomedical Engineering - Ingegneria Biomedica

Author: Vanessa Cannizzaro

Advisor: Prof. Elena De Momi

Co-advisor: Xiu Zhang

Academic year: 2023-2024

1. Introduction

Transoesophageal Echocardiography (TEE) is a medical imaging technique that uses ultrasound (US) waves to produce highly detailed images of the heart's structure and major blood vessels from a close proximity of a few millimetres, without interference from the lung and skeleton. TEE involves inserting a flexible, tendon-driven endoscope (gastroscope tube) with an US transducer at its tip into the esophagus (Fig. 1). The handle enables the insertion and rotation of the probe, as well as the control of the flexion of the distal bending section using two knobs. TEE is a valuable diagnostic tool for identifying various cardiac conditions, including congenital heart disease, cardiac masses, stroke, aortic pathologies, and valve abnormalities. It is also useful for monitoring cardiac procedures, such as transcatheter valve repair or replacement. During surgical procedures, TEE can be used in combination with X-ray fluoroscopic imaging to track surgical instruments, such as catheters. However, the use of fluoroscopy presents a significant challenge, as sonographers are exposed to ionizing radiation during the procedure. In addition, sonographers are at risk of occupational hazards due to the repetitive movements they perform for extended periods, combined with the use of protective equipment for radiation protection. These hazards can include musculoskeletal disorders. Finally, although TEE is a valuable tool, interpreting images and manipulating probes can be challenging. Especially in developing countries and small clinics, there is often a lack of readily available experts with the specialized skills required for TEE acquisition. To address the limitations of manual procedures, previous works have introduced a robotic approach. Shuangyi et al. developed a robotic sys-

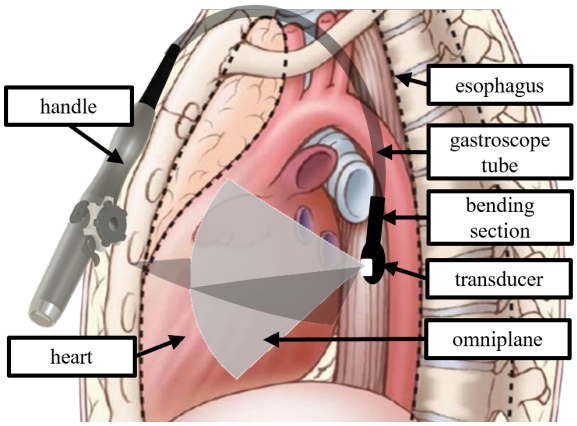

Figure 1: Sagittal view of the TEE examination

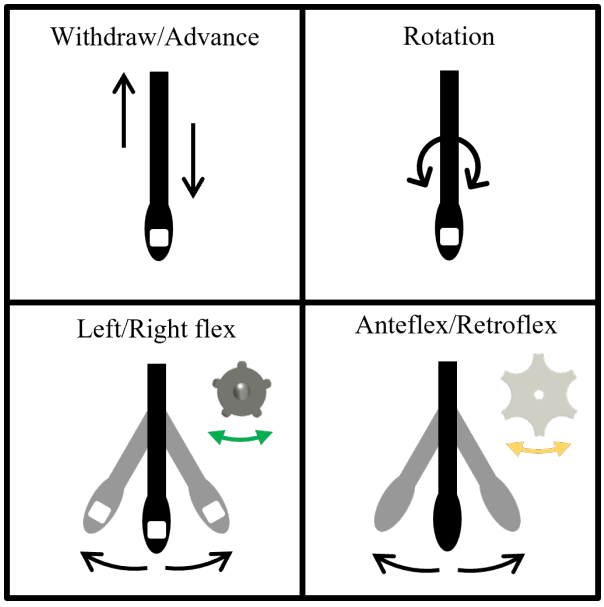

Figure 2: Terminology used to describe manipulation of the TEE probe, including all 4 DoF

tem and kinematic model for autonomous control of a commercial TEE probe [5]. Mostafa et al. presented a teleoperated robotic system that uses a compliant manipulator with soft actuators to guide the gastroscope tube [4]. Seyed et al. have introduced a robotic-assisted TEE system capable of controlling six degrees of freedom (DoF). The system is designed to maintain the gastroscope tube at an optimal inclination angle to minimize deflection [3].

Despite these advancements, non-linear hysteresis introduced by the tendon-driven mechanism remains a significant challenge. The hysteresis effect is produced by the inherent flexibility of the TEE probe and friction between tendons and the gastroscope tube. For this problem errors may occur during the procedure, since it's difficult to predict how proximal commands on the handle will affect distal motion of gastroscope tube. Several studies have attempted to address hysteresis and improve the performance of surgical robots that use a tendon-driven mechanism. Lee et al. proposed a simplified piecewise linear model to predict the non-linear hysteresis curve of Intra-cardiac Echocardiography (ICE) catheter and a practical method for calibration using motor current [2]. Due to the complexities involved in modelling such systems, researchers are increasingly turning to data-driven approaches. Long Short-Term Memory Neural Networks (LSTM) are gaining popularity in this regard, as they can incorporate sequential data for model learning. However, LSTM models require extensive training data to achieve optimal performance [1, 6].

The main contribution of this work is to present a new actuation system and control method for a commercial TEE probe (Philips, X7-2t, Netherlands) that can effectively address the issue of hysteresis effect. The proposed control method (Task Space Control) is innovative as it utilizes inverse kinematics of the robot and a hysteresis compensation model to control the position of the probe's tip. The compensation model is based on a simple offline calibration procedure and B-Splines approximation for the hysteresis curve. The newly developed B-Splines model for hysteresis compensation is compared with a piecewise linear approximation, as proposed in [2], to demonstrate its effectiveness. Finally, the mechanical design of the new robotic probe allows for easy detachment of the probe for sterilization, cleaning, or manual use.

2. Materials and Methods

This section describes the mechanical design of the robot, which actuates four DoF and allows for easy disassembly for cleaning and sterilization of the probe. It also explains Task Space Control and how it overcomes the limitation of unknown relationships between proximal commands and distal movements. The calibration procedure for hysteresis modeling and compensation, applied in Task Space Control, is then presented and discussed.

2.1. Design

The proposed TEE add-on robot can manipulate four DoF, as shown in Fig. 2: probe translation for insertion, probe rotation around the handle axis, medio-lateral (ML) bending (controlled by the upper knob), and antero-posterior (AP) bending (controlled by the lower knob). The handle control structure actuates ML and AP bending through two spur gear mechanisms (Fig. 3 A) and two servomotors (Dynamixel XM430-W350-R), one for each knob. The upper mechanism (green) controls ML bending, while the lower mechanism (yellow) controls AP bending. Each gear mechanism consists of a gear and a disc. The gear is attached to the motor's shaft, while the disc has an internal profile that mates

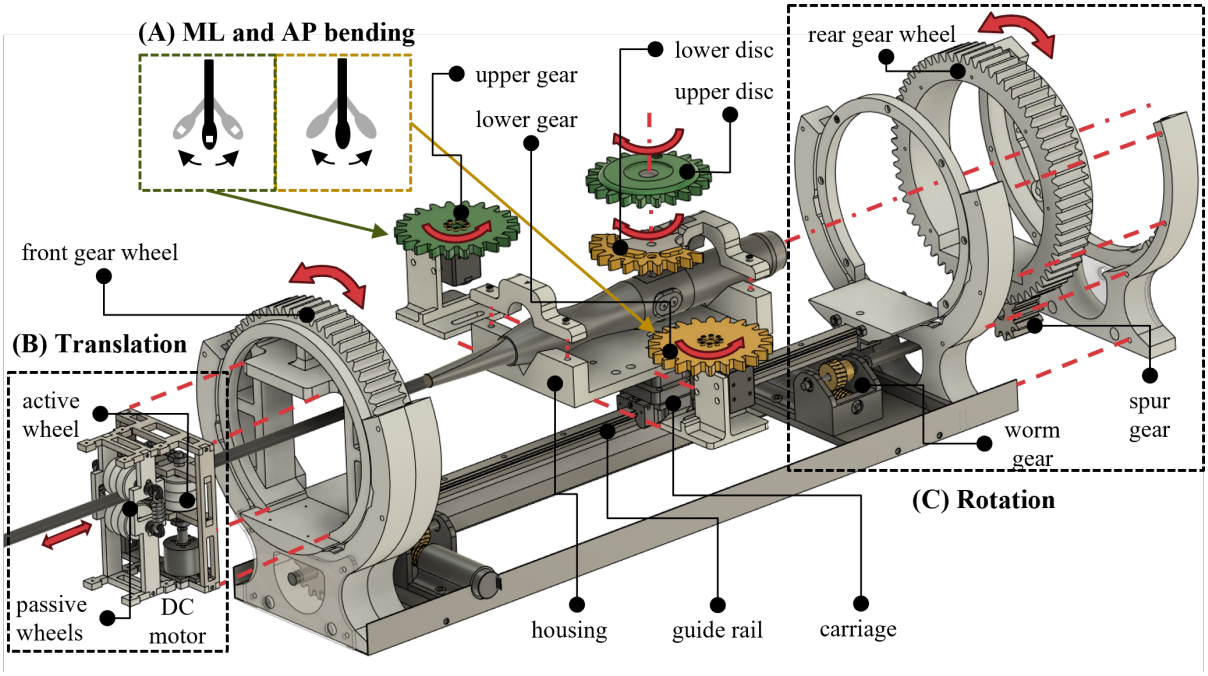

Figure 3: Schematic of mechanical assembly of the robotic TEE system: (A) Spur gear mechanisms for bending; (B) Translation module shows the spring-loaded conveyor roller with four wheels; (C) Rotation modules consist of a pair of worm gear and spur gear.

with the knob and an external profile that mates with the gear. This way, the motor's torque is transmitted to the knobs with a 1:1 transmission ratio. The TEE probe handle is placed in the V-shaped housing, which is secured by two clamps to prevent any movement. Two supports for the Dynamixel servomotors are attached to the housing. To prioritize user convenience for post-use cleaning and sterilization of the TEE probe, we have enabled easy detachment of the probe from the device.

The handle and bending mechanism are integrated with a driver that enables both translation and rotation of the probe. The design of the translation mechanism securely holds the insertion tube using rollers. The translation module (Fig. 3 B) consists of a spring-loaded conveyor roller with four wheels positioned at a 90°-degree angle. Three of these wheels are passive, while one acts as an active crankshaft. The DC-gearmotor (Faulhaber Series 2619S006SR 361 : 1, Germany) is connected to the active crankshaft. The TEE probe handle is held by a carriage that moves along a guide rail. The rotation around the axis is achieved using two spur gear wheels, one at the rear and one at the front (Fig. 3 C). The translation module is located within the front wheel. Two servomotors (Faulhaber Series 2250S024BX4 SC, Germany) and two worm gear mechanisms (one for the rear wheel and one for the front wheel) are used to drive this module.

2.2. Control

The Robotic Operating System (ROS) in Ubuntu is used as the central platform (master) to simultaneously control the four DoF, as shown in Fig. 4. The Dynamixel motors for AP and ML bendings interface with the U2D2 Power Hub using the RS485 protocol. The U2D2 acts as an intermediary, converting instructions from ROS into control signals for the motors and is connected to the PC via USB. The NI multifunctional I/O device is utilised to regulate three Faulhaber motors, one for translation and two for rotation, through PID control implemented in LABVIEW software. The UDP communication protocol facilitates seamless data exchange between the PC running ROS and the PC executing LABVIEW. Two Aurora 6-DoF electromagnetic (EM) sensors from NDI have been integrated at the tip and end (base) of the bending section to provide continuous, real-time position measurements. The input signal can be sent using either a joystick controller or a holographic interface.

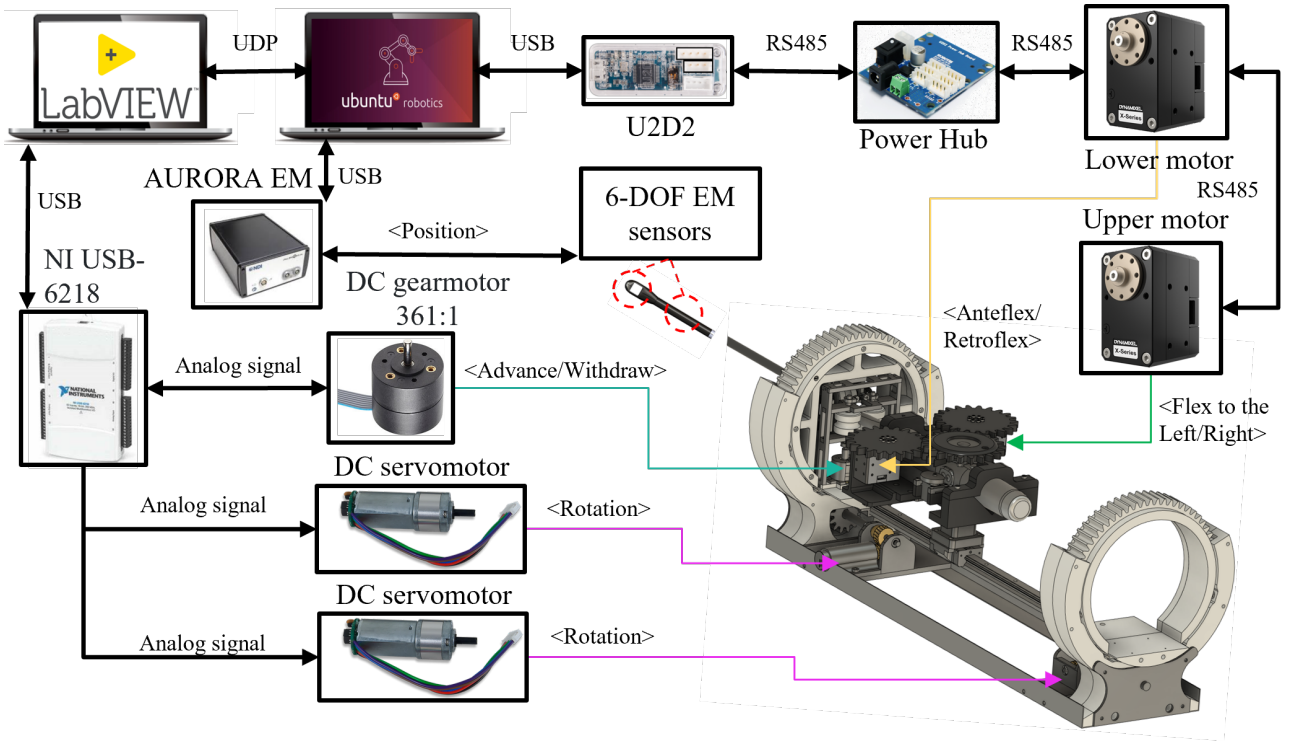

Figure 4: The robot's four DoF can be simultaneously controlled using a PC running ROS as the master device, connected to a PC running LABVIEW for translation and rotation control. The schematic illustrates the communication between ROS and the actuators.

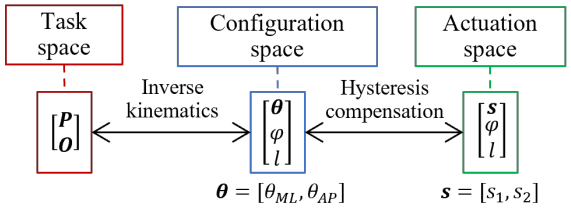

Figure 5: Task Space Control aims to establish the appropriate relationship between the distal movement of the probe's tip (task space) and proximal commands (actuation space) by utilizing inverse kinematics and hysteresis compensation.

This work presents Task Space Control, a new control method that aims to overcome the limitations of the unknown relationship between proximal commands and distal movements of the tendon-driven robot. Task Space Control allows for direct control of the position of the probe's tip (task space, Fig. 5), which is determined by the position of the tip P and base O of the bending section in space. Inverse kinematics is used to calculate the configuration space needed to achieve a particular pose. This space includes bending angles θ_{ML} and θ_{AP}, translation distance l, and rotation angle ϕ of the entire probe. However, it is unclear how the bending angles θ_{ML} and θ_{AP} are related to the Dynamixel motor positions s_1 and s_2 that control the bending, due to the hysteresis phenomenon affecting the tendon-driven TEE probe. Therefore, it is necessary to perform hysteresis analysis and compensation to determine the relationship between the actuation space and configuration space, as they differ from each other. Inverse kinematics and hysteresis compensation are explained in Section 2.3.

2.3. Hysteresis compensation

Previous research modelled the kinematics of the TEE probe's bending section using constant curvature theory [3, 5], as shown in Fig. 6 A. This theory suggests that the bending section, denoted as B, assumes a constant curvature within the bending plane, forming an arc characterised by an intersection angle, α (Fig. 6 A). By projecting this arc onto two orthogonal planes, specifically the AP and ML planes, two projected bending angles can be derived: θ_{AP} and θ_{ML}. The bending angles can be calculated based on established spatial relationships using

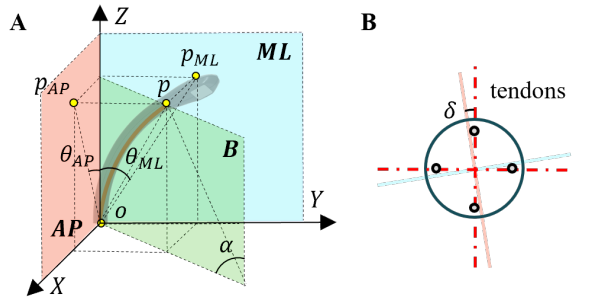

Figure 6: TEE probe geometry: (A) Kinematics of the TEE probe; (B) Cross-section of the TEE probe.

the following mathematical definition:

$$\theta_{ML} = \arccos\left(\frac{p_z}{\|p_{ML}\|}\right)$$
$$\theta_{AP} = \arccos\left(\frac{p_z}{\|p_{AP}\|}\right) \quad (1)$$

However, the probe's bending planes may twist in relation to where the tendons are attached due to errors from manufacturing and fatigue over time. To address this misalignment, a calibration process is essential for identifying and correcting the deviation angle, δ (Fig. 6 B). This step involves an optimization process in which the tendons are assumed to act independently on the bending section, and the ML bending range is symmetric. Moreover, a constraint is set to guarantee that the two bending planes AP and ML are perpendicular. To model the hysteresis phenomenon, a dataset is collected from the workspace using two EM sensors attached to the base and tip of the bending section, as shown in Fig. 4. Data was collected by applying sinusoidal input signals with four different periods and two distinct amplitudes to each motor, in order to investigates the relationship between the hysteresis effect and the motor rotation frequency and bending amplitude. During the data acquisition phase, the motor steps, s_1 and s_2, were recorded using the motors' integrated encoders. Simultaneously, precise measurements of the tip position, P, and the base position, O, are measured by the EM sensors. The position data is converted into two bending angles, θ_{AP} and θ_{ML}, by projecting the tip position, P, onto the bending planes, using equations 1. To implement compensation, the hysteresis cycle was modelled using B-Splines to map bending angles θ_{ML} and θ_{AP} with motor positions s_1 and s_2. The model returns the motor steps necessary to reach the desired bending angle θ based on the direction of movement (positive or negative). The model was then compared with a simplified piecewise linear approximation, similar to the one developed by Lee et al. [2].

3. Experiment

An experimental setup, as the one in Fig. 4 was developed to collect and analyse data on the hysteresis effect. ROS was used as the central platform to combine and synchronise signals from motors and sensors in our system.
The first experiment aimed to validate the hysteresis compensation model. A sinusoidal input signal with a changing frequency (two different frequencies, two periods for each frequency) was used to generate the desired bending angles $\theta_{ML,d}$ and $\theta_{AP,d}$. Hysteresis compensation is applied and actual bending angles $\theta_{ML,r}$ and $\theta_{AP,r}$ are computed. Errors E_{ML} and E_{AP} at each time step are computed as follows:

$$E_{ML} = |\theta_{ML,d} - \theta_{ML,r}|$$
$$E_{AP} = |\theta_{AP,d} - \theta_{AP,r}| \quad (2)$$

A second experiment was conducted to assess the ability of Task Space Control to follow a desired trajectory. Two circular trajectories passing through points in the acquired workspace were inputted. The error at each point of the trajectory is determined by computing the difference between the desired and actual tip position P_r and P_d:

$$E = |P_d - P_r| \quad (3)$$

4. Results

The probe is able to follow the sinusoidal input. Although the average error of the linear model (0.5°) is acceptable, it shows significant dispersion, with the maximum error reaching 1.5° for the AP bending angle. The error for the B-Splines model was always less than 1° in the AP direction and less than 0.7° in the ML direction. Median percentage error for B-Splines model is approximately 2% for AP and 1% for ML bending. The results of statistical analysis indicate that the difference between Linear and B-Splines model is statistically significant, at 5%

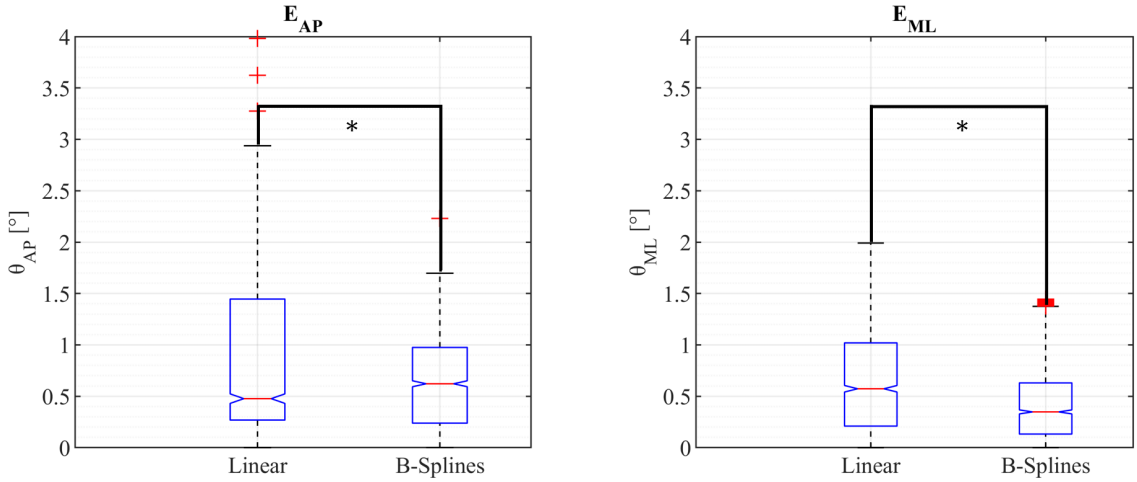

Figure 7: Error analysis shows better performance of B-Splines model for hysteresis compensation ($*, p - value < 0.05$).

confidence level (Fig. 7). For trajectory following validation of Task Space Control, two circular trajectories are defined. For each trajectory, inverse kinematics and hysteresis compensation are applied using both models (Linear and B-Splines). The robot is capable of following the intended trajectory with a median positional error E of approximately 3 to 3.5 mm, corresponding to 2.5% of the total length of the trajectory.

Table 1: The median positional error for trajectory following was calculated for both Linear and B-Spline models.

	Trajectory 1	**Trajectory 2**
$\mathbf{E_{Linear}}$	0.32 cm	0.35 cm
$\mathbf{E_{BSplines}}$	0.31 cm	0.33 cm

5. Discussion and Conclusion

The newly developed robotic probe for TEE can perform four movements: translation, rotation, anteroposterior (AP) bending, and mediolateral (ML) bending. The robotic probe can be controlled using either a joystick controller or a holographic interface as an input device. The four DoF are controlled simultaneously using the ROS platform. Following the calibration procedure, a B-Splines model was used to model and compensate the hysteresis. The B-Splines model can compensate for the hysteresis phenomenon characteristic of the bending, even at different movement velocities. The B-Splines model outperforms the linear piecewise approximation: Linear model is effective only for linear movements but fails when there is a change in direction due to backlash hysteresis. To perform Task Space Control, inverse kinematics and hysteresis compensation were applied, using the desired tip position as input. The experiment results show that the robot can follow a circular trajectory within the workspace with a median positional error of approximately 3 mm. This error is considered acceptable for the application, as a tip movement in the order of millimeters does not significantly affect the resulting image.

6. Limit and Future Work

The aim of Task Space Control was to compensate for non-linearities in tendon-driven bending and to establish the relationship between motor position and bending angle in both the mediolateral and anteroposterior directions. However, inverse kinematics for rotation and translation were not tested. Closed-loop control may be required for rotation due to plastic torsion, which causes the rotation of the handle to differ from that of the tip in a constrained environment. Closed loop control is recommended for real world applications as it can compensate for external disturbances. This can be achieved by using EM sensors to register the tip of the probe. However, the present work does not address the issue of the lack of force feedback, which remains a limitation of TEE examinations. The amount of force exerted by the tip on the oesophagus is unknown, which increases the risk of lesions

and perforations, the main complications associated with this procedure. In addition, the implementation of autonomous tasks for frequently repeated movements performed by sonographers could benefit from a more realistic trajectory. In this scenario, the sonographer would supervise the autonomous robot and input the desired trajectories to perform precise examinations.

References

[1] Dongchan Kim, Hongmin Kim, and Sangrok Jin. Recurrent neural network with preisach model for configuration-specific hysteresis modeling of tendon-sheath mechanism. *IEEE Robotics and Automation Letters*, 7(2):2763–2770, 2022.

[2] Dong-Ho Lee, Young-Ho Kim, Jarrod Collins, Ankur Kapoor, Dong-Soo Kwon, and Tommaso Mansi. Non-linear hysteresis compensation of a tendon-sheath-driven robotic manipulator using motor current. *IEEE Robotics and Automation Letters*, 6(2):1224–1231, 2021.

[3] Seyed MohammadReza Sajadi, Kim Mathiassen, Henrik Brun, and Ole Jakob Elle. Design, kinematic modeling, and validation of a robotic-assisted transesophageal echocardiography system. In *2022 IEEE/SICE International Symposium on System Integration (SII)*, pages 250–257. IEEE, 2022.

[4] Mostafa Sayahkarajy and Ahmad Athif Mohd Faudzi. Design of a mechatronic interface with compliant manipulator for robot assisted echocardiography. In *Journal of Physics: Conference Series*, volume 2107, page 012005. IOP Publishing, 2021.

[5] Shuangyi Wang, James Housden, Davinder Singh, Kaspar Althoefer, and Kawal Rhode. Design, testing and modelling of a novel robotic system for trans-oesophageal ultrasound. *The International Journal of Medical Robotics and Computer Assisted Surgery*, 12(3):342–354, 2016.

[6] Di Wu, Yao Zhang, Mouloud Ourak, Kenan Niu, Jenny Dankelman, and Emmanuel Vander Poorten. Hysteresis modeling of robotic catheters based on long short-term memory network for improved environment reconstruction. *IEEE Robotics and Automation Letters*, 6(2):2106–2113, 2021.